



Agricultural By-Products as Green Chemistry in Elimination of Reactive Red 43 from Aqueous Media- Adsorption Properties and Thermodynamics Study

Heba M. El Refay, Asrar Goma, Nagwa Badawy and Fatema Al Zahra Ghanem



CrossMark

Department of Chemistry, Faculty of Science (Gils), Al-Azhar University (Girls), Yousef Abbas Str,
P.O. Box: 11754, Nasr City, Cairo, Egypt.

Abstract

The aim of this study is to find an effective green waste (GW) natural material as an adsorbent for the removal of C.I. Reactive Red 43 (RR43) from an aqueous solution using batch experiments. Agricultural-by-products such as Peanut Shell (PS) and Corn Cobs (CC) have been used as (GW). Scanning electron microscopy (SEM) coupled with Energy Dispersive X-ray (EDX) and Fourier transform infrared spectrometer (FTIR) techniques were used to characterize the adsorbent before and after adsorption process. The influence of operating factors such as adsorbent dose, initial concentration of dye, contact time, pH solution and temperature were studied. The equilibrium data was analyzed by Langmuir and Freundlich isotherm models and showed a good fit with the Freundlich isotherm ($R^2=0.999$). Batch kinetic data were analyzed using pseudo-first order and pseudo-second order kinetic models, the adsorption kinetics data were fitted to pseudo-second order kinetic model with a good agreement with the intra-particle diffusion model. The parameters of thermodynamic including enthalpy ΔH° , entropy ΔS° and free energy ΔG° demonstrated that the adsorption process was feasible, spontaneous, and exothermic in nature. The results clarified that a large percentage removal, and the optimized conditions were $(7.6 \pm 0.2$ and $4.3 \pm 0.2)$ solution pH for PS and CC respectively, 20mg/L initial dye concentration, adsorbent dose 0.1 gm/20 ml, and 90 min adsorption time. 80.46% and 86.76% of dyes were removed by PS and CC respectively at experimental optimum conditions. These agricultural by-products are renewable, biodegrade able, inexpensive, and easily accessible with little or no cost. Their application as adsorbents is in line with the current trend of green chemistry and green environmental policies.

Keywords: Reactive Red 43 (RR43), Low-Cost adsorbents, Adsorption Isotherm, Kinetic, Thermodynamic

1. Introduction

Dyes are known to be toxic and persistent compounds in the environment [1], the latter are mainly classified in to anionic, cationic, and nonionic dyes, indeed, the toxicity of cationic dyes is higher than that of anionic dyes. [2]. Pollution from industrial discharges is currently receiving particular attention worldwide. Nowadays, there are more and more cases of ecosystem alterations and public health problems that can lead to the elimination of living species (plants, animals, humans).

Numerous studies have shown that certain dyes are responsible for several diseases [3-5] and can cause skin irritation, allergic dermatitis, kidney, central nervous system, liver, and brain dyes functions [6,7] and can also cause cancer and mutations. As a result, not only is efficiency in the removal of organic materials from wastewater vital in the selection of a

suitable technique in terms of the environment and economy, but also the required raw materials and costs play a critical role. Reactive dyes are very toxic and harmful for living and aquatic life. They may cause cancer, skin diseases, and allergic reactions [8-10].

Besides the toxic, mutagenic, and carcinogenic effect, the presence of reactive dyes causes aesthetic damage to water bodies, increases water turbidity, and reduces the penetration of light through water. Adsorption, unlike the other technique, could be a potential alternative for removing dyes from aqueous solution due to its efficiency, high selectivity, low cost, ease of operation, and implicitly, availability under a wide range of experimental settings, among other advantages [11,12]. All of these benefits, however, are dependent on the nature of adsorbent material utilized in the adsorption processes of dye. As a result, a commonly available adsorbent material with

*Corresponding author e-mail: hebaelrefay.5919@azhar.edu.eg

Receive Date: 25 October 2021, Revise Date: 01 January 2022, Accept Date: 05 January 2022

DOI: 10.21608/ejchem.2022.102614.4757

©2022 National Information and Documentation Center (NIDOC)

a simple preparation technique will boost the adsorption process' benefits and will advocate this method for possible widespread use.

As a result, numerous studies in recent years have revealed the possible use of agricultural by-products and industrial wastes in the manufacture of adsorbents. Many agricultural by-products, such as rice wine lees [13] corn cob and sapota seed powder [14], banana peels [15], on peanut hull [16], etc., have been examined for their absorptive capabilities as inexpensive adsorbents. The goal of this study is to determine the potential of PS and CC native as green waste (GW) for the removal of reactive red 43 (RR43) dye from a solution. PS and CC may be used as dye adsorbents because of their chemical compositions, which included a large quantity of cellulose, pectin, hemicellulose, and lignin, as well as a variety of polar functional groups such as hydroxyl, carboxylic, and phenolic acid groups. [17-19].

The aim of this research is to use agricultural waste by-product as GW to removal of RR43 dye from aqueous media by PS and CC as adsorbent. The effect of variables such as dose of adsorbent, initial dye concentrations, solution pH, contact time, and temperature on dye removal efficiency from aqueous solution was investigated. The adsorption and removal mechanism of PS and CC on the RR43 were discussed by fitting the isothermal adsorption equation and kinetic equation, the pseudo-first order and pseudo-second-order models were used to investigate the adsorption kinetics. Langmuir and Freundlich isotherm models were used to analyses the equilibrium data. The adsorption's thermodynamic characteristics were also studied, which may provide a new idea for wastewater treatment from toxic azo dye by PS and CC as adsorbent.

The application of the adsorption method to the process of removing polluting organic ions from wastewater, rather than the most common separation process in current research, is novel in this study, and the removal process is characterized by ease of implementation, like the adsorption process.

2. Materials and Methods

2.1. Sorbent

with the goal of valuing agricultural waste, a less economical and effective support for dye retention is being examined. This study suggests natural supports which are the local as (PS) and (CC), this adsorbent is prepared by firstly washed with distilled water to remove the surface adherent particles and water-

soluble components impurities. Then it's dried with the exposure of the sun light, in order to eliminate de humidity and facilitate crushing. After that, were dried in an oven at 105°C to remove moisture and enable grinding. The dried slices were crushed and sieved to a particle size range of 0.315 mm before being kept in a dissector for further use. A portion of the solid support is chemically activated.

2.2. Materials

The C.I. Reactive Red 43 dye was supplied from Sigma–Aldrich company, Egypt. The characteristics of the dye are listed in Table (1). All chemicals used in the adsorption experiments were purchased from Merck and used without further Purification. The de ionized water was used for preparation of dye stock solution. The dye stock solution was prepared by dissolving 1 gm of dye in 1000 ml of double distilled water to give the concentration of 1000 mg/L. The pH value of the working solutions was adjusted to the desired values by using 0.1 M HCl or 0.1 M NaOH.

2-3. Batch Experiment

The influence of several variables on the sorption of RR43 was studied, including initial concentration of dye, contact time, adsorbent dose, and temperature. Batch adsorption experiments with a known mass of adsorbent and 20 ml of dye solution were carried out in 250 ml Erlenmeyer flasks under an isothermal shaker (30±1°C) and agitation speed 250 rpm. The suspended particles in each sample were then filtered, and the dye concentration in the supernatant was determined using a double beam UV–Vis Spectrophotometer at 5.7 nm. The amount of adsorption capacity (q_e) and percentage of adsorption were calculating as follows:

Removal (%R) is calculated from the formula.

$$\%R = \frac{C_0 - C_e}{C_0} \times 100 \quad (1)$$

The optimum time is obtained from the plot adsorption capacity versus time using the formula:

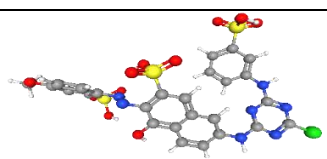
$$q_t = \frac{(C_0 - C_t)V}{W} \quad (2)$$

Also the equilibrium time for the adsorption of the dye is obtained using the formula;

$$q_e = \frac{(C_0 - C_e)V}{W} \quad (3)$$

Where C_0 , C_t and C_e represent the initial, time and equilibrium concentrations of the dye (mgL^{-1}), respectively and w is the weight of the adsorbent (g), where V is the volume of dye solution (L).

Table (1): Some of Physical Properties of C.I. Reactive Red 43.

Dye name	IUPAC name:	Mol. formula	Mwt	λ max	Structure formula
RR43	trisodium;2-[[6-[[4-chloro-6-(3-sulfonatoanilino)-1,3,5-triazin-2-yl] amino]-1-oxido-3-sulfonaphthalen-2-yl]diazinyl]-5-methoxybenzene sulfonate	$C_{26}H_{17}ClN_7Na_3O_{11}S_3$	804.07	5.3 nm	

3. Results and Discussion

3.1. Sorbent Characterization:

3.1.1. Scanning Electron Microscopy (SEM)

Scanning electron microscopy (SEM) was used to examine the morphological characteristics of (PS and CC) adsorbent. SEM images of the adsorbent surface before and after adsorption tests are shown in Figure (1). The porous and rough structure of the adsorbent is easily recognized in Figures (1a and b) which is very advantageous for adsorption applications. The surface structure of sorbent changed after dye adsorption, as observed in Figures (1c and d). On the surface of dye-adsorbed, the rippled and rough surface became a smoother and tighter structure, proving the effective adsorption of dye via a stable dye layer on the surface of adsorbent material.

3.1.2 Energy Dispersive X-ray (EDX)

The percentage weight of chemical compositions available on the surface was determined using an Energy Dispersive Spectrometer (EDX) analysis for PS and CC as adsorbents before and after the RR43 adsorption procedure, as shown in Figure (2). The results are organized in the table below. Figure (2), show, EDX analysis of sorbent according to table; the biggest levels corresponded to the PS and CC, as well as oxygen, demonstrating the adsorbent's organic nature.

3.1.3. Fourier Transform Infrared Spectroscopy (FTIR)

The functional groups present on the PS and CC surfaces were identified using FTIR spectra. Figures (3 and 4) shows that the broad overlapping band at 3421 cm^{-1} can be attributed to $\nu(\text{O-H})$ groups contained in lignin, cellulose and hemicelluloses. The band observed at 2921 cm^{-1} is assigned to asymmetric C-H band. The two strong absorption peaks in 1737 and 1624 cm^{-1} was assigned to carbonyl C=O stretching (present in esters, aldehydes, ketones groups and acetyl derivatives) and C=C, respectively [20,21]. These all-bands changes after adsorption as shown in Figure (4). Sorption peaks at 3421 changed to 3436 cm^{-1} , 1737 to 1460 cm^{-1} and 542 to 539 cm^{-1} which may be due to functional process of RR43 dye on PS and CC adsorbent [22].

3.2. Point of Zero Charge (pHpzc)

The pH_{ZPC} of Gw was determined by using the batch equilibration method. This technique is dependent on the H^+ or OH^- from an aqueous media are adsorbed onto the surface of Gw. Depending on the pH of the solution and the characteristics of Gw, the groups on the surface of Gw can either accept or donate an additional proton from the solution. The surface of GW becomes positively charged by accepting of protons from the acidic solution; by contrast, it becomes negatively charged due to the loss of protons in a basic solution.

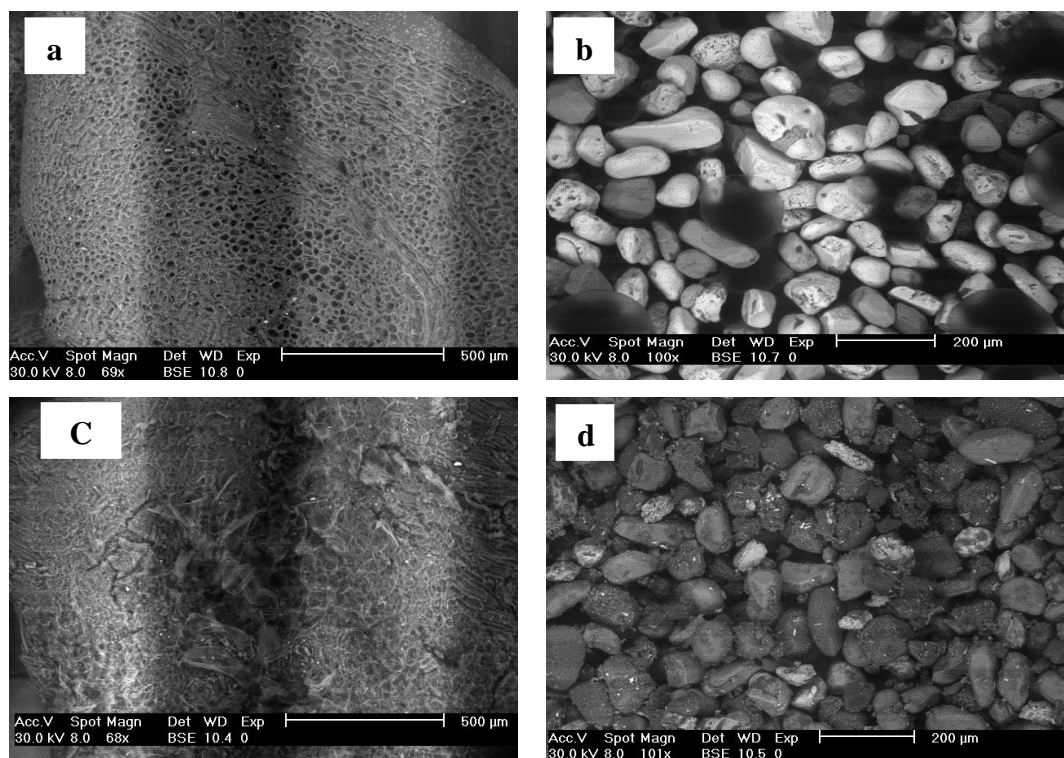


Fig. 1: SEM Images of (a) PS, (b) CC before adsorption of RR43 and (c)PS, (d) CC after adsorption process

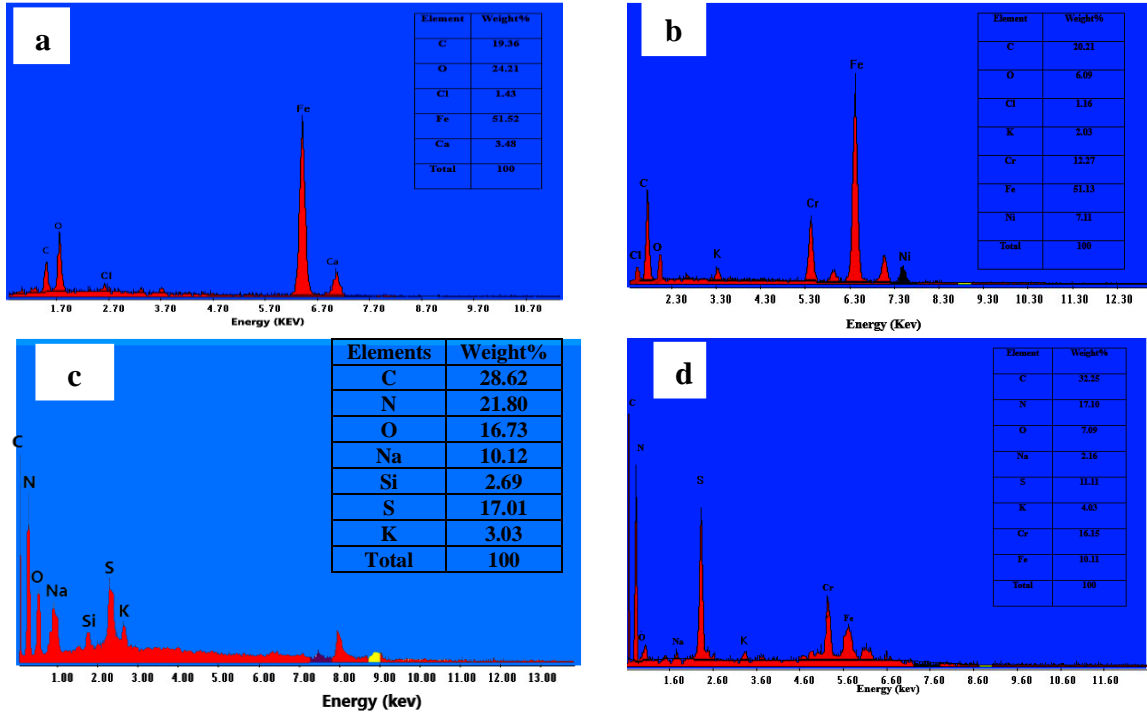


Fig. 2: EDX for (a) PS, (b) CC before adsorption of RR43 and (c) PS, (d) CC after adsorption process

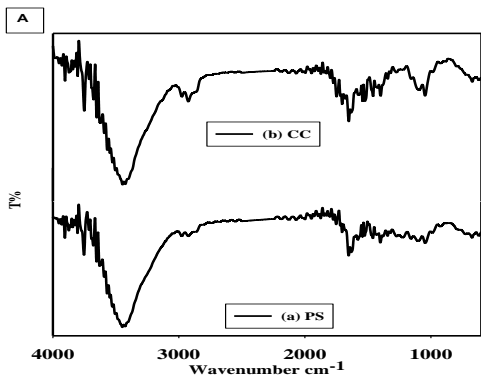


Fig. 3: FTIR spectra for (A) PS and CC before adsorption.

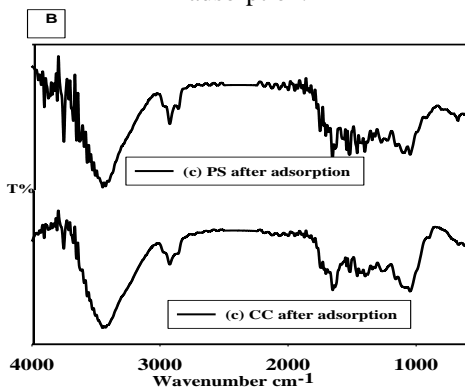


Fig. 4: FTIR spectra for (B) PS and CC after adsorption.

The pH at which the surface of Gw is neutral is known as pH_{ZPC} [23,24]. the pH_{ZPC} of PS was determined to be 7.3 as show in

Figure (5), The adsorbent surface is negatively charged at $pH > pH_{ZPC}$, preventing negatively charged reactive dye molecules from adsorbing due to electrostatic repulsion. As a result, RR43 adsorption onto PS is favoured at pH lower than 7.6, while the pH_{ZPC} value for raw CC adsorbent being 4.3. Based on this finding, it can be concluded that basic alteration of the adsorbate resulted in a negative (basic) surface charge for the adsorbent.

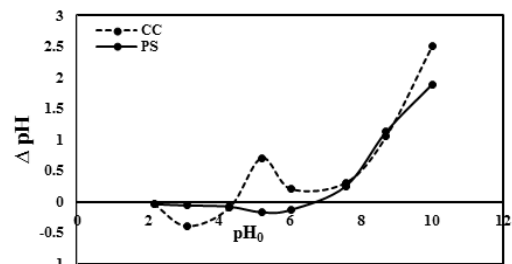


Fig. 5: zero-point charge of CC and PS adsorbents

3.3. Effect of Different Adsorption Parameters

The surface plots from the model help to observe the influence of four variables (pH solution, initial concentration of dye, adsorbent dose, and time) on the removal of dye.

3.3.1. Interaction Effect of pH Solution and Initial Concentration of Dye

The influence of pH on RR43 sorption from aqueous solution was investigated in this work by changing the initial pH of the solutions from 2 to 12 by adding a few drops of diluted NaOH or HCl, with initial concentrations of 20, 30, 40, 50, and 60 mg/L of dye. Figure (6) shows that the adsorption efficiency decreased when pH solution increased from 2 to 10. On the other hand, at low pH solution, the dye exists predominantly in the molecular form and the electrostatic interaction between positively charged surfaces of bio sorbents and molecules of dye will be also suppressed. However, a further increase in pH resulted in the worsening of dye removal efficacy. The pH_{ZPC} for PS and CC was established as 7.6 and 4.3, respectively. Above these values, the surfaces of tested bio sorbents are negatively charged. Thus, the worsening of dye removal with increasing pH could be attributed to the weakness of electrostatic interaction between anionic reactive dye and active sites of bio sorbent. While increasing the solution pH ($pH > 2.1$) with increasing the initial concentration of dye resulted in a significance reduction in

the percentage removal. The removal percentage of RR43 declined as the initial concentration of dye increased, as shown in the figure. This can be explained by the fact that when the initial concentration of dye rises, the interaction between PS and CC with RR43 becomes more intense. [25]

3.3.2. Interaction Effect of Initial Concentration of Dye and Contact Time

As demonstrated in Figure (7), adsorption at various concentrations of dye was rapid at first, but then steadily decreased as adsorption progressed until equilibrium was attained. This is due to the fact that the adsorption sites were initially unoccupied and highly accessible, allowing RR43 molecules to quickly engage with them. Thus, the removal percentage was found to be 80.46% and 86.76% for PS and CC adsorbent respectively at 20 mg/L of initial concentration of dye, while at 60 mg/L this value reduced to 54.68 % and 59.4 % by both adsorbents. The results showed that the sorption capacity did not change after 90 min; hence 90 min was chosen as the agitation time for isotherm studies

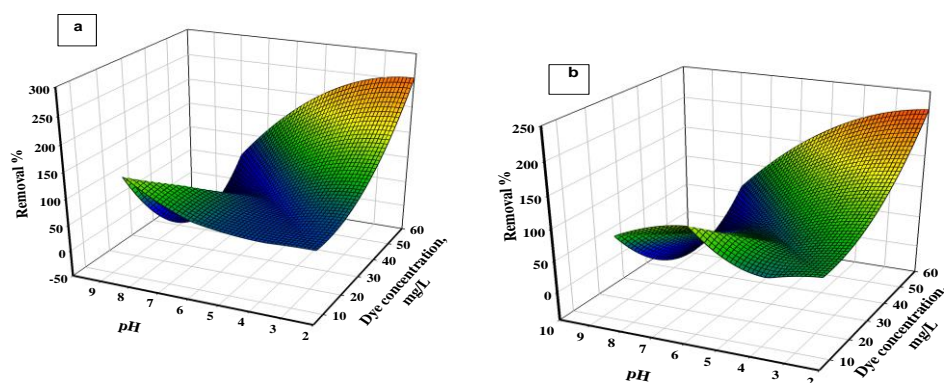


Fig. 6: 3D plot of interaction effect of solution pH and initial concentration of dye on adsorption of RR43 by (a) PS, and (b) CC.

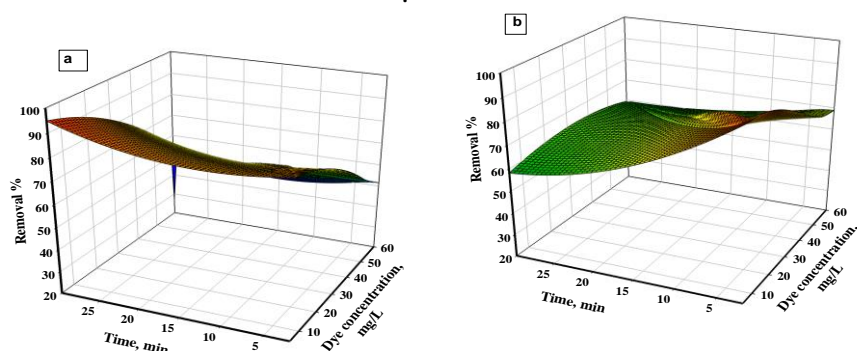


Fig.7: 3D plot of the interaction influence of initial concentration of dye and contact time on removal % RR43 by (a) PS and (b) CC.

3.3.3. Interaction Influence of Adsorbent Dosage and Initial Concentration of Dye

Figure (8) may be noted that as the adsorbent dose was increased and the concentration of dye was decreased, removal of dye increased. The results are displayed in Figure 8, which demonstrates a significant increase in the amount adsorbed as the adsorbent dose is increased. The saturation of the adsorbent's active sites can be explained by the increase in the quantity of dye molecules and the difficulty of adsorbent-adsorbate interaction, which explains the saturation of the adsorbent's active sites. However, it was noted that when the adsorbent dose increased, the rate of dye removal percentage dropped marginally. Because there was more adsorbent in the dye solution, resulting in the distances between the adsorbent particles were reduce, leaving numerous binding sites unoccupied. [26].

3.3.4. Temperature Effect

Temperature influences on adsorption were studied by altering the temperature from 30 to 50 °C as show in Figure (9). The percentage removal of RR43 decreased from 73.64 % and 76.1 % by PS and CC to 67.81% and 70.17 % respectively, with a temperature increase from 30°C to 50°C, indicating that

high temperatures are detrimental to the adsorption process. On the other hand, as the temperature of the range investigated rises, the sorption capacity of RR43 diminishes, revealing that the RR43 adsorption on the PS and CC is exothermic in nature, and the low temperature promotes adsorption. This effect could be caused by dye molecules being released from the bio sorbent into the aqueous solution as the temperature rises. A similar result has also been reported [27].

3.4. Adsorption Isotherms

Adsorption isotherms are quite useful in explaining the adsorption mechanism. The Langmuir and Freundlich isotherms are the most commonly used models in adsorption evaluation. The Langmuir isotherm enables estimation of the maximum adsorption capacity on the assumption that the surface of the adsorbent is covered with a monolayer of adsorbed molecules. By applying the Freundlich model, it is possible to estimate the adsorption intensity assuming that the adsorbent surface is heterogeneous and multilayer sorption occurs. The linearized form of the Langmuir and Freundlich equations are given as following.

A mathema

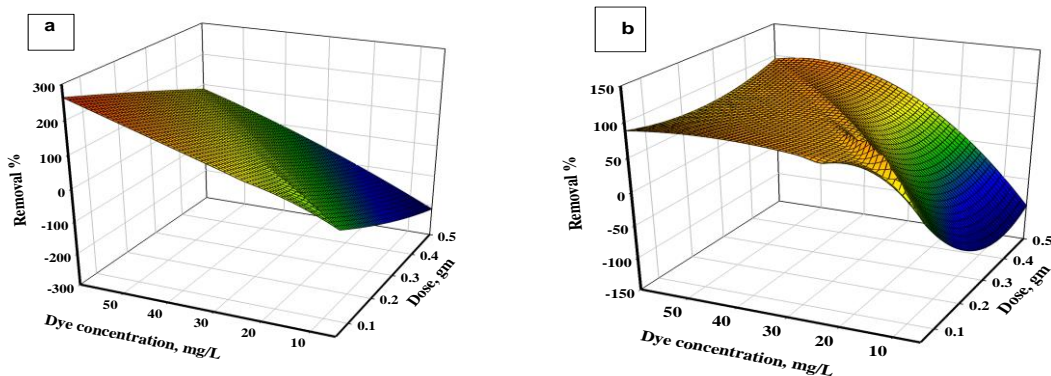


Fig. 8: 3D plots the interaction effect of adsorbent dose and initial dye concentration on adsorption of RR4³⁺ by (a) PS and (b) CC.

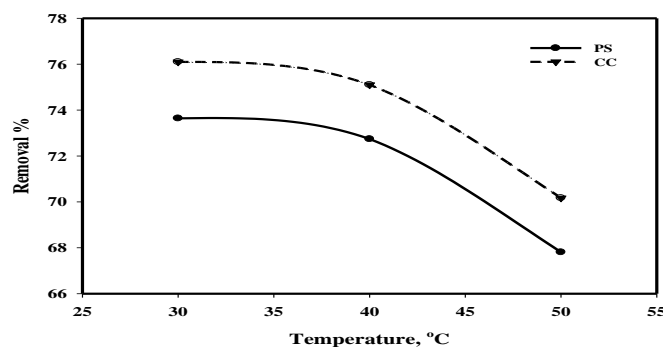


Fig. 9: Temperature effect on removal % of RR43 by PS and CC at dose :0.1g/20 ml, solution pH 7.6 for PS and 4.3 for CC, and contact time 90min.

tical expression of the generalized non-linear form of the Langmuir isotherm is given by:

$$\frac{C_e}{q_e} = \frac{C_e}{q_{\max}} + \frac{1}{K_L q_{\max}} \quad (4)$$

The dimensionless constant separation term (R_L) was used to study the form of the Langmuir isotherm in order to detect high affinity adsorption. R_L was calculated as follows:

$$R_L = \frac{1}{(1 + K_L C_0)} \quad (5)$$

Where, C_0 is the initial concentration of dye (mg/l), R_L indicates the type of isotherm to be irreversible ($R_L = 0$), favorable ($0 < R_L < 1$), linear ($R_L = 1$) or unfavorable ($R_L > 1$) [28].

Freundlich isotherm represents adsorption equilibrium and is widely used and was chosen to measure the adsorption intensity of the adsorbate on the adsorbent surface. The following equation expresses the isotherm, which is an empirical equation that can be used to explain heterogeneous systems [29]. The logarithmic form of equation is often used to fit batch equilibrium data [30].

$$\log q_e = \log K_f + 1/n \log C_e \quad (6)$$

where q_{\max} (mg/g) is the maximum sorption capacity corresponding to complete monolayer coverage and K_L (L/mg) is the Langmuir constant. K_f is the Freundlich constant ((L/mg) related to the sorption capacity and the constant n is related to adsorption intensity. The constants isotherm calculated from the slope and the intercept from Figures (10 and 11). The calculated isotherm constants together with correlation coefficients (R^2) for both models are presented in Table (2).

3.5. Adsorption Kinetics:

The kinetic order of RR43 sorption onto the natural adsorbent was determined using 0.1g/20ml of adsorbent at RR43 concentrations

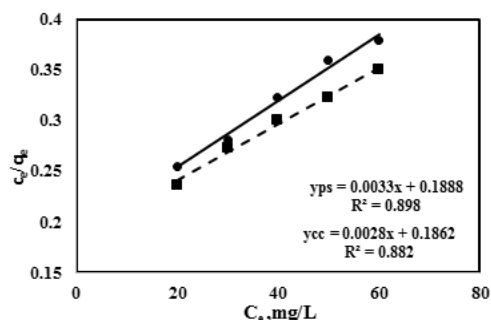


Fig. 10: The Langmuir isotherm model by PS and CC

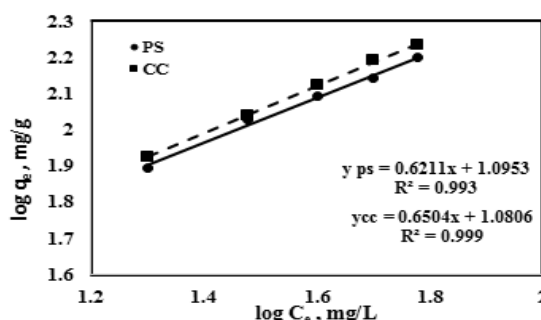


Fig. 11: The Freundlich isotherm model by PS and CC

of 20, 30, 40, 50, and 60 mg/L, an adsorption time of 2-120 min, and the optimum pH and temperature. The experimental data was described using two kinetic models: pseudo-first order and pseudo-second order. Lagergren proposed the model of the first order. [27], it is given by the following linear equation.

$$\frac{dq_t}{dt} = k_1(q_e - q_t) \quad (8)$$

Where q_e and q_t (mg. g⁻¹) are the amounts of dye adsorbed at equilibrium and at time (t) minute, respectively; and k_1 (min⁻¹) is the pseudo-first-order rate constant. After integration by applying boundary conditions $q_e = 0$ at $t = 0$ and $q_t = q_t$ at $t = t$, the equation becomes:

$$\log (q_e - q_t) = \log q_e - k_1 t \quad (9)$$

Whereas if pseudo-first-order kinetic model is used, the plot of $\ln (q_e - q_t)$ versus t yields a straight line, and the slope and intercept can be used to calculate the rate constant k_1 and the amounts of dye adsorbed at equilibrium q_e . [31] A pseudo-second-order model, which is commonly used in adsorption, was proposed. The following is the shape of this model:

$$\frac{dq_t}{dt} = k_2 (q_e - q_t)^2 \quad (10)$$

Where K_1 (min⁻¹) and K_2 (g.mg⁻¹.min⁻¹) are the velocity constants for two kinetic models respectively, and q_e (mg. g⁻¹) is the adsorbed amount at equilibrium for two kinetic models, q_t (mg. g⁻¹) is the adsorbed amount at any time, t (min) is the contact time. The obtained values for the kinetic constants as well as the correlation factors of the two models are shown in the following Table (3). The results are also plotted as shown in Figures (12a and b) and it is obvious that the sorption kinetics of the RR43 onto PS and CC, supports are well explained by the pseudo second order model for both of bio sorbents.

Table (2). Linearized Langmuir and Freundlich Isotherms Constant for PS and CC.

parameter Adsorbents	Langmuir Isotherm				Freundlich Isotherm		
	K_L (L/mg)	q_m (mg/g)	R_L	R^2	K_f (L/mg)	n	R^2
PS	0.018	303.03	0.975-0.992	0.988	12.45	1.610	0.993
CC	0.015	357.14	0.979-0.993	0.992	12.04	1.538	0.999

The second-order rate constants were used to calculate the initial sorption rate, H , (mg/g. min), given by:

$$H = k_2 q_e^2 \quad (11)$$

Table (3), Fitting the experimental data to pseudo-second order kinetics yielded better correlation coefficients (R^2) than fitting the experimental data to pseudo-first order kinetics for all the systems studied. As a result, the sorption was more favourably by pseudo-second order kinetic model, which assumed that the rate limiting step may be chemisorption involving valency forces through sharing or exchange of electrons between sorbent and sorbate [32,33].

The normalized deviation (ND) and normalized standard deviations (NSD) were estimated utilizing equation for error analysis using equation [21].

$$NSD = 100 \sqrt{\frac{\sum \left(\frac{q_e(\text{exp}) - q_e(\text{cal})}{q_e(\text{exp})} \right)^2}{n}} \quad (12)$$

$q_e(\text{exp})$ and $q_e(\text{cal})$ are experimental and predicted RR43 uptake (mg/g) respectively, where n is the number of observations made. The following Table (3) shows the obtained values for the kinetic constants as well as the correlation factors for the two models. The pseudo second-order rate constant k_2 of the dye adsorption is expressed as a function of temperature by Arrhenius relationship using the Equation:

$$\ln k_2 = \ln A - \frac{E_a}{RT} \quad (13)$$

Where R is the gas constant, T is the absolute temperature in ($^{\circ}\text{K}$) and E_a activation energy, The value of E_a is calculated as 14.02 and 13.34 kJ/mol for PS and CC respectively from the slope of plot of $\ln k_2$ versus $1/T$ which explained as Figure (13). The type of adsorption mechanism is determined by the value of E_a ($\text{kJ}\cdot\text{mol}^{-1}$). If E_a is between 8 and 16 $\text{kJ}\cdot\text{mol}^{-1}$, the adsorption process is regulated by a chemical mechanism, but if $E_a < 8 \text{ kJ}\cdot\text{mol}^{-1}$, the adsorption process is controlled by a physical mechanism [22]. The determined values of E_a indicated that dye adsorption occurs through chemical adsorption. This established that chemisorption is predominantly operating force along. Chemisorption, in which valency forces are engaged via electron sharing or exchange between the adsorbent and the adsorbate, may be the rate-limiting phase. The time-dependent data from this investigation was then used to see if intra-particle kinetics played a role in the adsorption of RR43 ions from their aqueous solutions as well [34]. It is proposed that the adsorption process' diffusion mechanism and rate-controlling phases be identified. According to this theory

$$q_t = k_{id} t^{0.5} + C \quad (14)$$

where k_{id} is the rate constant of intra-particle diffusion ($\text{mg}\cdot\text{g}^{-1}\cdot\text{min}^{1/2}$) and C ($\text{mg}\cdot\text{g}^{-1}$) is a constant that indicates the thickness of the boundary layer; it has been shown that the larger the value of C , the greater the effect of the boundary layer [24]. When the k_{id} values for the macropore and micropore diffusion stages for RR43 ions are compared, it becomes clear that the micropore diffusion stage is the rate limiting phase. This is because the RR43 ions' micropore diffusion constant k_{id2} was smaller than the macropore diffusion constant k_{id1} . This demonstrates that the slower and rate-determining stage is micropore diffusion. Table (3) further reveals that the boundary layer effect, i.e., the intercepts of the second lines from the plots in Figures (12c), has a bigger effect at the micropore diffusion stage than at the macropore diffusion stage at different temperatures.

6. Adsorption Thermodynamics

The following equations can be used to calculate thermodynamic parameters such as Gibbs free energy ΔG° , enthalpy ΔH° and entropy ΔS° at different temperatures, 30, 40 and 50 $^{\circ}\text{C}$.

$$\ln K_d = \frac{\Delta S^{\circ}}{R} - \frac{\Delta H^{\circ}}{RT} \quad (15)$$

$$\Delta G^{\circ} = \Delta H^{\circ} - T \Delta S^{\circ} \quad (16)$$

Where $K_d = q_e/C_e$ is the distribution coefficient, R is the universal gas constant and T is the temperature in (K). The values of ΔG° , ΔH° , and ΔS° were calculated by plotting the Figure (14) and are listed in Table (4). This result indicated that the magnitudes of Gibbs free energy practically remained constant during the adsorption process. The negative ΔG° values show that the RR43 adsorption processes on PS and CC are feasible and spontaneous. The negative value of ΔH° suggests that the adsorption process is exothermic and chemical in character, involving significant forces of attraction between RR43 molecules and PS and CC [35]. The positive ΔS° value indicates the increased randomness at the solid- liquid interface during the fixation of the RR43 on the active sites of the studied adsorbent.

4. Conclusion

This study focuses on using agricultural by-products for as biological adsorbent for the removal of dyes from aqueous environments which is extremely practicable and in vogue with the current popularity of green chemistry and green environmental practices. Agricultural waste such as unmodified PS and CC powders as adsorbents can be effectively used for the removal of RR43 by adsorption. SEM, EDX, FTIR and pH_{ZPC} were used to characterize the synthesized material.

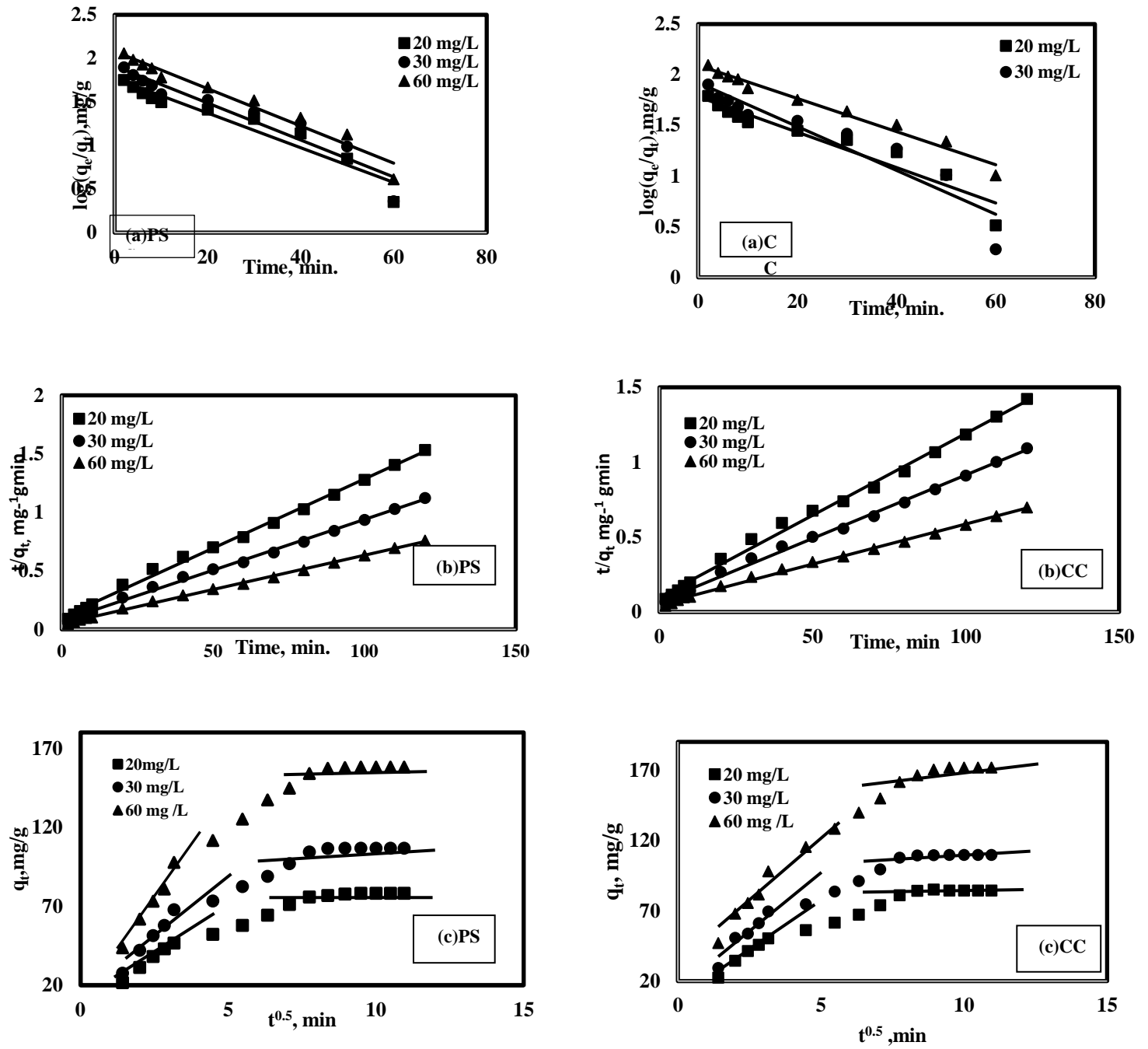


Fig. 12: (a) Pseudo-First-order kinetic, (b) Pseudo-Second-order kinetic and (c) Intraparticle Diffusion dye at concentration 20 mg/L, 30 mg/L and 60 mg/L for adsorption of the RR43 onto PS and CC.

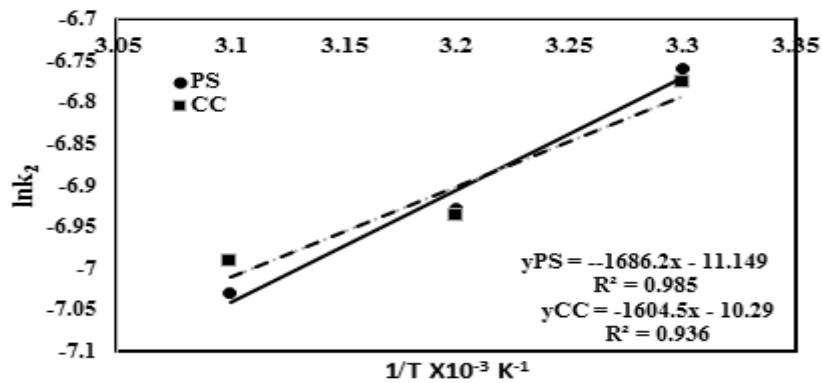


Fig. 13: Plot of $\ln K_2$ Vs $1/T$ for the adsorption of RR43 onto (PS and CC).

Table (3): Summarize the Kinetics Models Constant and Correlation Coefficient for Adsorption of Reactive Dye onto PS and CC at Different Concentrations.

Adsorbent	Conc. mg/L	Pseudo- First- order			Pseudo-Second- order					
		k_1 min ⁻¹	q_e (cal) mg/g	R^2	k_2 min ⁻¹	q_e (exp.) mg/g	q_e (cal.) mg/g	H	NSD	R^2
PS	20	0.046	58.97	0.931	1.36×10^{-3}	78.21	84.75	9.768	0.976	0.997
	30	0.049	81.70	0.916	1.05×10^{-3}	106.7	114.9	13.87	1.018	0.992
	60	0.049	120.3	0.962	7.33×10^{-4}	108.1	169.5	21.06	0.978	0.999
CC	20	0.040	60.63	0.919	1.20×10^{-3}	83.33	91.74	10.10	1.006	0.996
	30	0.050	83.43	0.854	1.07×10^{-3}	109.7	117.7	14.81	0.942	0.997
	60	0.038	123.8	0.975	5.60×10^{-4}	171.8	185.2	19.21	1.026	0.997
Intraparticle diffusion model										
k_1	C_1	R^2	k_2	C_2	R^2					
14.45	1.946	0.994	4.054	38.83	0.839					
22.24	3.315	0.995	5.144	57.01	0.828					
29.25	2.138	0.984	6.946	90.92	0.828					
15.70	1.722	0.987	4.628	39.39	0.849					
21.27	2.473	0.949	5.425	57.24	0.825					
26.68	10.78	0.966	9.049	82.74	0.897					

Table (4): Thermodynamic Parameters of RR43 on PS and CC at Different Temperatures

Temp. °C	30	40	50	ΔH° (kJ/mol)	ΔS° (kJ/mol)
PS	ΔG° kJ/mol)			-11.34	0.015
	-15.89	-16.04	-16.19		
CC	-16.44	-16.58	-16.72	-12.20	0.014

This biosorption mechanism was largely dependent on the basic pH, with a favourable pH (7.6 ± 0.2 and 4.3 ± 0.2) solution pH for PS and CC respectively, 20mg/L initial dye concentration, adsorbent dose 0.1 gm/20 ml, and 90 min adsorption time. resulting in the highest clearance rate, 80.46% and 86.76% of dyes were removed by PS and CC respectively at experimental optimum conditions. The biosorption capability improved as the initial concentration of dye was increased. The Freundlich isotherm matched the experimental results nicely. Pseudo-first order, pseudo-second order, and intraparticle diffusion models were used to investigate adsorption kinetics. The results show that the system's adsorption mechanisms follow pseudo-second order kinetics. Thermodynamic analysis confirmed that adsorption was a physisorption process. Finally, these results show that PS and CC can be employed as an effective and economical adsorbent for the treatment of synthetic dye-containing wastewaters.

Conflicts of interest

“There are no conflicts to declare”.

Formatting of funding sources

No funding sources

5. References

1. Wu Y., Pang H., Liu Y., Wang X., Yu S., Fu D., Chen J. and Wang X., Environmental remediation of heavy metal ions by novel-nanomaterials: A review. *J. Environ. Poll.*, 12, 246-608 (2019).
2. Rajabi M., Mahanpoor K. and Moradi O., Preparation of PMMA/GO and PMMA/GO-Fe₃O₄ nanocomposites for malachite green dye adsorption: Kinetic and thermodynamic studies. *J. Compos. Part B Eng.*, 167, 544-555 (2019).
3. Zohre S., Atallah S.G. and Mehdi A., Experimental study of methylene blue adsorption from aqueous solutions onto carbon nano tubes. *J. Int. Reso. Environ. Eng.*, 2, 16-28 (2010).
4. Ahmed A.A. and Hameed B.H., Fixed bed adsorption of reactive azo dye onto granular

- activated carbon prepared from waste. *J. Hazard. Mater.*, 175, 298-303 (2010).
5. Uddin M.T., Rakunuzzaman M. Khan M.M. and Islam M.A., Adsorption of MB from aqueous solution by jak fruit (*Artocarpus hetero pyllus*) leaf powder: Fixed bed column study. *J. Environ. Manage.*, 60, 3443-3450 (2009).
 6. Alok M., Gupta V. K., Arti M. and Jyoti M., Process development for the batch and bulk removal and recovery of a hazardous, water-soluble azo dye (Metanil Yellow) by adsorption over waste materials (Bottom Ash and De-Oiled Soya). *J. Hazard. Mater.*, 151, 821-832 (2008).
 7. Haik Y., Shahnaz Q., Ashley G., Sarmadia A., and Reyad S., Phase change material for efficient removal of crystal violet dye. *J. Hazard. Mater.*, 176, 1110-1112 (2010).
 8. Lellis B., Fávoro-Polonio C.Z., Pamphile J.A., Effects of textile dyes on health and the environment and bioremediation potential of living organisms. *J. Bio. technol. Res. Inn.*, 3, 275-290 (2019).
 9. Aziz E.K., Abdelmajid R., Rachid L.M. and Mohammadine E.H., Adsorptive removal of anionic dye from aqueous solutions using powdered and calcined vegetables wastes as low-cost adsorbent. *J. Arab. Basic Appl. Sci.*, 25, 93-102 (2018).
 10. Ahmed A.E., Removal of reactive dye from aqueous solutions using orange and lemon peel as bio-adsorbent, *Int. J. Sci. Res. Eng. Tech.*, 5, 542-548(2020).
 11. Anastopoulos I. Margiotoudis I. and Massas I., The use of olive tree pruning waste compost to sequester methylene blue dye from aqueous solution, *Int. J. Phyto. mediation.*, 20, 831-838 (2018).
 12. Li Q., Tang X., Sun Y., Wang Y., Long Y., Jiang J. and Xu H., Removal of rhodamine B from wastewater by modified *Volvariella volvacea*: batch and column study. *J. RSC Adv.*, 5, 25337-2534 (2015).
 13. Qian W., Liping L., Gangliang T., Qiaole M. and Xu M., Adsorption of Azo Dye Malachite Green onto Rice Wine Lees: Kinetic and Adsorption Isotherms. *J. Int. Quart. Sci.*, 19, 563-570 (2020).
 14. Das M. P., Kanika P. G., and Jeevitha L., Optimization of Malachite Green Dye Adsorption by Corn Cob and Sapota Seed. *J. Int. Knowledge Press.*, 20, 1302-1308 (2020).
 15. Santosh S., Amit K. and Himanshu G., Activated banana peel carbon: a potential adsorbent for Rhodamine B decontamination from aqueous system. *J. Appl. Water Sci.*, 10, 185 (2020).
 16. Mühendislik D., Dergi P., Tarafından Y. and Tüm H. S., Congo Red Removal from Aqueous Solutions by Adsorption on Peanut Hull. *J. Eng. Sci. and Res.*, 2, 28 - 35(2020).
 17. Someya K. Yoshiki S. and Okubo Y., Antioxidant compounds from bananas (*Musa Cavendish*). *J. Food Chem.*, 79, 351-354 (2020).
 18. Sulaiman A. Yusoff S. F., Eldeen N. A. M., Seow I. M., Sajak E. M. and Ooi K. L., Correlation between total phenolic and mineral contents with antioxidant activity of eight Malaysian bananas. *J. Food Compos. Anal.*, 24, 1-10 (2011).
 19. Emaga M. Robert T.H., Ronkart C., Wathélet S.N., Paquot B., Dietary fiber components and pectin chemical features of peels during ripening in banana and plantain varieties. *J. Bio. Res. Tech.*, 99, 4346-4354 (2008).
 20. Taşar S., Kaya F. and Özer A., Biosorption of lead (II) ions from aqueous solution by peanut shells thermodynamic and kinetic studies. *J. Enviro. Chem. Engin.*, 2, 1018-1026 (2014).
 21. Somasekhara R., Sivaramakrishna L. and Varada R. A., The use of an agricultural waste material, Jujuba seeds for the removal of anionic dye (Congo red) from aqueous medium. *J. Hazard. Mater.*, 203, 118-127 (2012).
 22. Sarma P.J., Kumar R. and Pakshirajan K., Batch and Continuous Removal of Copper and Lead from Aqueous Solution using Cheaply Available Agricultural Waste Materials. *J. Int. Enviro. Res.*, 9, 635-648 (2015).
 23. Cerovic L. S., Milonjic S. K., Todorovic M. B., Trtanj M. I., Pogozhev Y. S., Blagoveschenskii Y. and Levashov E. A., Point of zero charge of different carbides. *J. Colloids Surf. A: Phys. Eng. Aspects.*, 297, 1-6 (2007).
 24. Hashemian S., Salari K. and Yazdi Z. A., Preparation of activated carbon from agricultural wastes (almond shell and orange peel) for adsorption of 2-Pic from aqueous solution. *J. Indus. Eng. Chem.*, 20, 1892-1900(2014).
 25. Khan S., Ali T. A., Singh I., Sharma V. V., Utilization of Fly Ash as Low-cost Adsorbent for the Removal of Methylene Blue, Malachite Green, and Rhodamine B Dyes from Textile Wastewater. *J. Envi. Prot. Sci.*, 3, 11-22 (2009).
 26. Nahali L., Miyah Y., Assila O., El Badraoui A., El Khazzan B. and Zerrouq F., Kinetic and thermo dynamic study of the adsorption of two dyes brilliant green and eriochrome black T using a natural adsorbent "sugarcane bagasse. *J. Mor. Chem.*, 7 715-726 (2019).
 27. Cheraghi E., Ameri E. and Moheb A., Continuous biosorption of Cd(II) ions from aqueous solutions by sesame waste:

- Thermodynamics and fixed-bed column studies. *Des. Water Treat.*, 2015, 12-74 (2015).
28. El Maguana Y., Elhadiri N., Bouchdoug M., Benchanaa M. and Jaouad A., Activated carbon from prickly pear seed cake: optimization of preparation conditions using experimental design and its application in dye removal. *J. Int. Chem. Eng.*, 2019, 1-12 (2019).
 29. Zhang F., Chen X., Wu F. and Yuefei J., High adsorption capability and selectivity of ZnO nanoparticles for dye removal. *J. Colloids and Surfaces A: Physicochemical and Engi. Aspects*; 509, 474:483 (2016).
 30. Ahmad R. Y., Gharib M., Mehdi T. R., Mohsen A., Shahram N., Meysam E. K. S., Mohammad K. and Maryam S. T., Using Egg shell in Acid Orange 2 Dye Removal from Aqueous Solution. *J. Iranian Health Sciences*; 3, 38:45 (2015).
 31. Patil V.S., Mandal S. and Mayadevi S., Alginate and hydrotalcite-like anionic clay composite systems: Synthesis, characterization, and application studies. *J. Micro por. Meso por. Mat.*, 158, 241:246 (2014).
 32. Augustine E., Sorptive removal of Methylene blue from aqueous solution using palm kernel fiber: Effect of fiber dose. *J. Bio. chem. Eng.*, 40, 8-18 (2008).
 33. Wang S. and Li H., Kinetic modeling and mechanism of dye adsorption on unburned carbon. *J. Dyes Pigments.*, 72, 308-314 (2007).
 34. Qingye S. and Linzhang Y., The adsorption of basic dyes from aqueous Solution on modified peat-resin particle. *J. Water Rese.*, 37, 1535-1544 (2003).
 35. Chen D., Chen J., Luan X., Ji, H. and Xia Z., Characterization of anion-cationic surfactants modified montmorillonite and its application for the removal of methyl orange. *J. Chem. Eng.*, 171, 1150-1158 (2011).
 36. Doma A.S., Nazly Hassan A. I. and Hesham M. A. Adsorption of Methylene Blue Dye on Hydrothermally Prepared Tungsten Oxide Nanosheets. *J. Egypt. Chem.*, 63,483-498 (2020).